GEOLOGY

Natural hydrogen in the volcanic-bearing sedimentary basin: Origin, conversion, and production rates

Quanyou Liu[1,2]*, Yongbo Wei[3,4]*, Pengpeng Li[1], Xiaowei Huang[1], Qingqiang Meng[5], Xiaoqi Wu[5], Dongya Zhu[5], Huiyuan Xu[5], Yin Fu[3,4], Di Zhu[6,7], Wang Zhang[3,4], Zhijun Jin[1]

The origins of natural hydrogen in natural gas systems of sedimentary basins and the capacity of these systems to store hydrogen remain inadequately understood, posing crucial questions for the large-scale exploration of natural hydrogen. This study reports on the natural gas composition, stable carbon and hydrogen isotopic values, and helium isotopic values of gas samples collected from the Qingshen gas deposit within volcanic rocks of the Songliao Basin. Natural hydrogen primarily originates from water radiolysis, water-rock interactions (WRI), and mantle. The Qingshen gas deposit contains 95.23 × 10^9 cubic meters of abiotic CH_4, of which 15.24 × 10^9 cubic meters was generated through hydrogen conversion via Fischer-Tropsch synthesis, with the maximum original hydrogen reserves calculated to be approximately 61.9 × 10^9 cubic meters. We estimated that the study area has generated a maximum total of 572 × 10^9 cubic meters of radiolytic hydrogen, 248 × 10^9 cubic meters of WRI hydrogen, and 127 × 10^9 cubic meters of mantle-derived hydrogen.

INTRODUCTION

In recent years, escalating global energy demands coupled with mounting environmental concerns have propelled hydrogen into the spotlight as an efficient and clean energy source (*1*). Although some believe that the prospects for hydrogen use across various industries may be poor (*2*), there is nevertheless a current need for clean hydrogen to replace gray or polluting hydrogen (steam reforming of methane). Natural hydrogen extracted directly from geological formations, a clean and economical method of hydrogen production, has been dubbed "golden hydrogen" or "white hydrogen" (*3*, *4*). "Hunt for natural hydrogen heats up" was recognized by *Science* as one of the "2023 Breakthroughs of the Year," underscoring its significance as a monumental scientific discovery and a pivotal trend for the future.

The geological formations of the natural world contain vast reserves of natural hydrogen, with the Precambrian continental lithosphere alone estimated to generate approximately 554 million tons of hydrogen annually (*5*). To date, the global scientific community has identified hundreds of natural hydrogen occurrences (*6*–*11*). In the context of natural hydrogen discoveries, the dominance of inorganic sources is evident, and high concentrations of natural hydrogen were primarily found in ore deposits, ophiolite belts, and deep basement rocks (*12*, *13*). For example, in Albania's Bulqizë ophiolite, degassing of serpentinized chromitite has been observed to release gas comprising up to 84% H_2, with an annual release estimated at no less than 200 tons (100 × 10^6 mol/year) (*9*).

Theoretically, the internal strata of sedimentary basins feature various traps capable of storing natural gas, suggesting a high likelihood of natural hydrogen being similarly trapped. This process is similar to that of petroleum and natural gas systems and can lead to the formation of hydrogen-rich natural gas reservoirs (*14*–*16*). However, the propensity for considerable natural hydrogen dissipation is attributed to the small size, high reactivity, and ease of diffusion of hydrogen molecules (*3*). Compared to regions with high concentrations of natural hydrogen, natural hydrogen concentrations in clastic rocks, volcanic rocks, and carbonate reservoirs within sedimentary basins are generally lower. The low concentration and reserves of geological hydrogen in geological structures present notable limitations for commercial exploitation, and it remains to be proven that proposed development projects can produce sufficient marketable quantities to attract potential buyers. Knowledge of natural hydrogen and efforts to develop the resource are still in the exploratory stages worldwide, with only the natural hydrogen reservoir in Mali, West Africa having been commercially developed (*17*). Natural hydrogen in sedimentary basins may have multiple origins (organic and inorganic or crustal and mantle) and undergo complex conversion processes (*11*, *12*, *18*–*22*). Therefore, in the complex geological settings of sedimentary basins, establishing and quantitatively evaluating the various origins and conversion processes of natural hydrogen in natural gas reservoirs are vital for discovering hydrogen-rich natural gas reservoirs. In addition, assessing the production rates of natural hydrogen from different origins and the store rates of natural hydrogen by natural gas reservoir systems will be instrumental in future natural hydrogen exploration in global sedimentary basins.

The Songliao Basin is a continental Mesozoic-Cenozoic sedimentary basin located in Northeast China. The Songliao Basin dominates the eastern part of the Songnen Block (Fig. 1A), which is a lithospheric block located within the eastern segment of the Central Asian Orogenic Belt. A collisional assemblage of microcontinents and multiple periods of magmatic activity occurred across this region during the development of the Palaeo-Asian Ocean subduction system in the late Palaeozoic [~350 to 250 million years (Ma)], the Mongolia-Okhotsk Ocean subduction system in the early Mesozoic (~250 to 200 Ma), and the (Palaeo-)Pacific Plate subduction system in the Meso-Cenozoic (<200 Ma) (*23*). The Qingshen gas deposit, the world's largest deep volcanic rock gas deposit, is

[1]Institute of Energy, School of Earth and Space Sciences, Peking University, Beijing 100871, China. [2]Northwest Institute of Eco-Environment and Resources, Chinese Academy of Sciences, Lanzhou 73000, China. [3]Key Laboratory of Deep Petroleum Intelligent Exploration and Development, Institute of Geology and Geophysics, Chinese Academy of Sciences, Beijing 100029, China. [4]University of Chinese Academy of Sciences, Beijing 100049, China. [5]Petroleum Exploration and Production Research Institute, SINOPEC, Beijing 100083, China. [6]School of Sustainable Energy and Resources, Nanjing University, Suzhou 215163, China. [7]Suzhou Grand Energy Technology Co. Ltd., Suzhou 215010, China.
*Corresponding author. Email: liuqy@pku.edu.cn, qyouliu@sohu.com (Q.L.); weiyongbo@mail.iggcas.ac.cn (Y.W.)

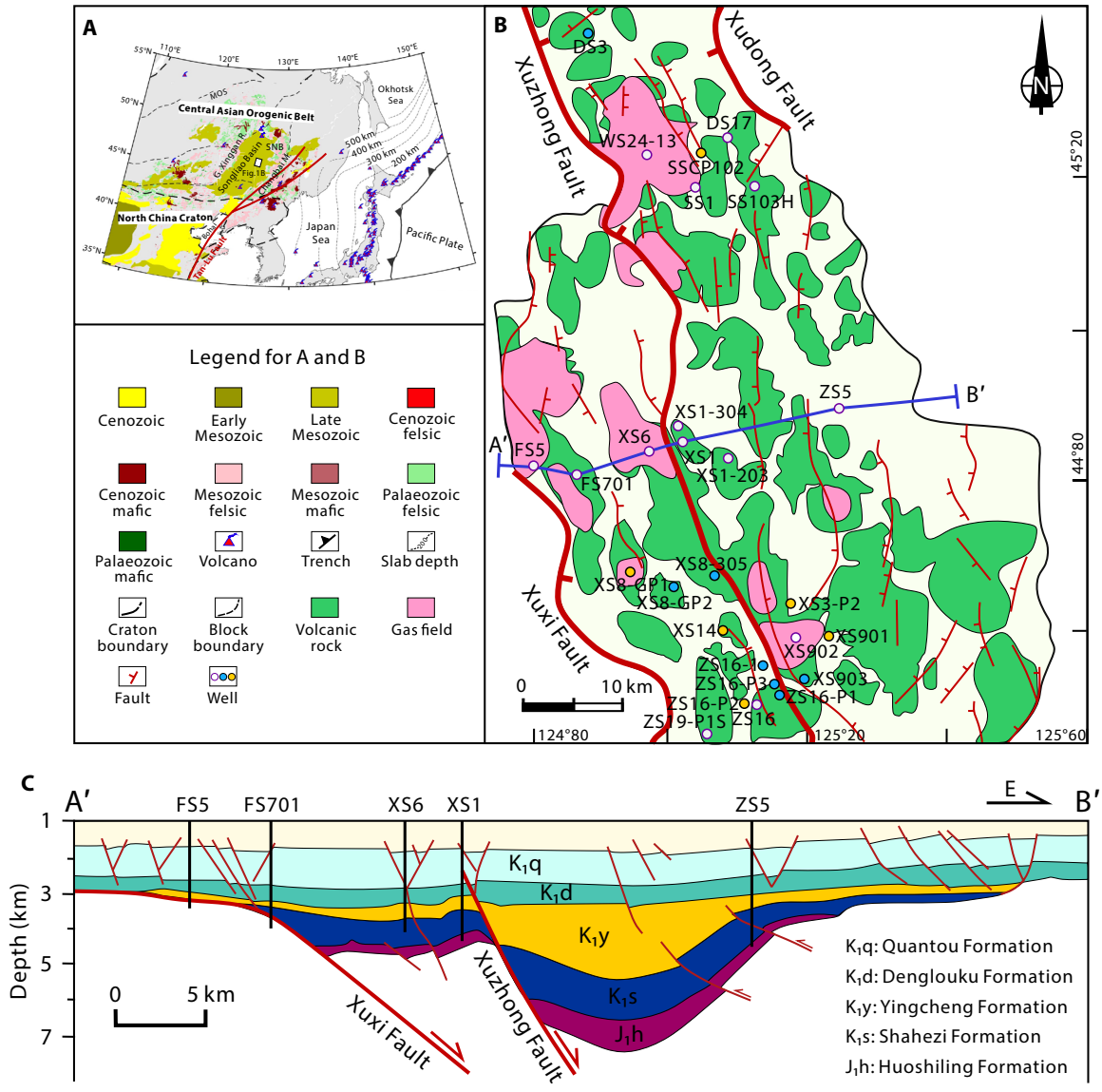

Fig. 1. Location and geological context for the study area. (**A**) Tectonics of East Asia and Songliao Basin, modified after (*23*). SNB, Songnen Block; MOS, Mongol-Okhotsk Suture. The yellow circles represent group I gases, while the blue circles represent group II gases. (**B**) Distribution of volcanic rocks and gas deposits of the Yingcheng Formation from the Xujiaweizi fault depression in the northern Songliao Basin, modified after (*75*). (**C**) Structural cross section of the Xujiaweizi rift depression, modified after (*76*).

located in the Xujiaweizi rift depression of the Songliao Basin (Fig. 1B) (*24*). The rift system is characterized by thick volcanic and clastic strata, including the Upper Jurassic Huoshiling Formation and the Lower Cretaceous Shahezi, Yingcheng, Denglouku, and Quantou Formations (Fig. 1C), with deep natural gas primarily accumulating in the volcanic rocks. The Songke 2 (SK2) well, located in the Xujiahuizi fault depression, is the world's first continental scientific drilling well to penetrate Cretaceous continental strata. It has revealed extensive continuous hydrogen gas anomalies in the Lower Cretaceous Denglouku and Yingcheng Formations and the basement rocks, with hydrogen concentrations ranging from 1.36 to 26.89% (*25*). Although the discovery of high concentrations of natural hydrogen during the drilling of the SK2 well demonstrated the hydrogen exploration potential of the deep formations in the Songliao Basin, the origin and conversion processes of hydrogen in industrial natural gas reservoirs require further investigation.

We obtained natural gas samples from 23 wells in the Qingshen gas deposit within the Xujiaweizi depression. On the basis of gas composition and carbon-hydrogen-helium isotope values (table S1), a crust-mantle mixed origin and conversion system for hydrogen in the volcanic-bearing sedimentary basin was established. We provided estimates of hydrogen production rates in the volcanic-bearing sedimentary basin and quantitatively assessed the natural gas system's ability to store natural hydrogen. This holds substantial implications for discovering and exploring natural hydrogen in sedimentary basins.

RESULTS

Characterization of natural gas composition

The 23 gas samples we examined exhibit variable molecular composition (table S1), with CH_4 content ranging from 74.61 to 97.09%

and CO_2 content ranging from 0.0018 to 22.68%. N_2 and He contents range from 0.53 to 8.61% and 99 to 600 parts per million (ppm), respectively. The concentration of natural hydrogen is relatively low compared to Mali and Kansas (*7*, *17*), ranging from 0 to 5.0%, with an average of 0.53%. The gas compositions of the Qingshen gas deposit within the Songliao Basin indicate that natural hydrogen primarily occurs in natural gas reservoirs dominated by CH_4, CO_2, and N_2. The weak correlation between hydrogen concentration and the contents of CH_4, N_2, CO_2, and He suggests that natural hydrogen does not have an identical genetic link to the four gases and may undergo a complex process of generation and conversion (Fig. 2).

Characterization of gas isotopes

We conducted carbon, hydrogen, and helium isotope testing experiments on the gas samples to better understand the origins of various gas components. The results show that $\delta^{13}C_1$, $\delta^{13}C_2$, and $\delta^{13}C_3$ values range between −32.5 and −25.0 per mil (‰) (averaging −27.8‰), −34.8 and −21.3‰ (averaging −30.7‰), and −34.8 and −20.8‰ (averaging −31.1‰), respectively. The differences in $\delta^{13}C$ among the C_1-C_3 alkanes (methane through propane) in some of the samples follow an "inverse" trend (fig. S1), i.e., $\delta^{13}C_1 > \delta^{13}C_2 > \delta^{13}C_3$, or opposite the usual pattern of increasing $\delta^{13}C$ with increasing carbon number (*26*). This carbon isotopic inverse feature may arise from factors including but not limited to the high maturity of the source rocks, cracking of heavy hydrocarbons, and mixing of gases from different sources (*27*). The $\delta^{13}C$-CO_2 values range from −13.2 to −3.9‰, with several samples exhibiting heavier isotopic characteristics (>−10.0‰), suggesting an inorganic origin for CO_2 (*28*).

The natural hydrogen extracted from gas samples shows a wide range of hydrogen isotope compositions (δ^2H), from −698 to −522‰, with an average of −599‰, which is significantly heavier compared to the δ^2H-H_2 values in sedimentary basins worldwide (e.g., Mali, Kansas, Witwatersrand Basin) (*7*, *17*, *29*). The δ^2H-C_1 versus δ^2H-H_2 cross-plot (Fig. 3) reveals two group gases with distinct data distributions: one with a positive correlation between δ^2H-C_1 values and δ^2H-H_2 values, and another where δ^2H-H_2 values are greater, while δ^2H-C_1 values are more dispersed. These two group gases are automatically separated at a δ^2H-H_2 value of −600‰, which is close to the −650‰ threshold proposed in (*13*) for distinguishing between mantle-derived and crust-derived hydrogen (Fig. 3). The reason for the difference in data distribution between the two groups gases may be that the hydrogen is dominated by different origins, as discussed in the following section.

The Qingshen gas deposit of the Songliao Basin has R/Ra values (where R is the ratio of $^3He/^4He$ and Ra is the atmospheric $^3He/^4He$ ratio, approximately 1.4×10^{-6}) ranging from 0.75 to 2.15, with an average of 1.47, indicating the presence of mantle-derived fluid

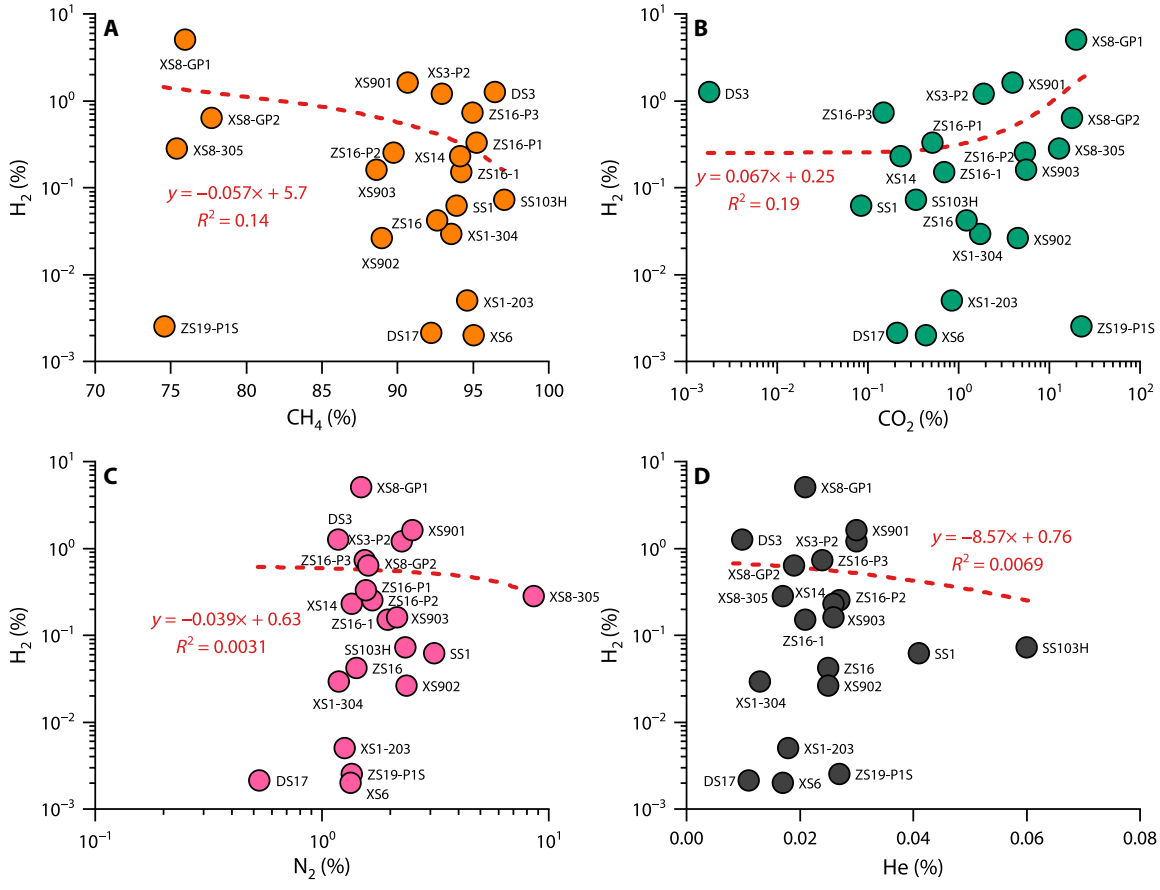

Fig. 2. Correlation of hydrogen concentration with CH_4, CO_2, N_2, and He concentrations for the Qingshen gas deposit, Songliao Basin. (**A**) Hydrogen concentration versus CH_4 concentration. (**B**) Hydrogen concentration versus CO_2 concentration. (**C**) Hydrogen concentration versus N_2 concentration. (**D**) Hydrogen concentration versus He concentration.

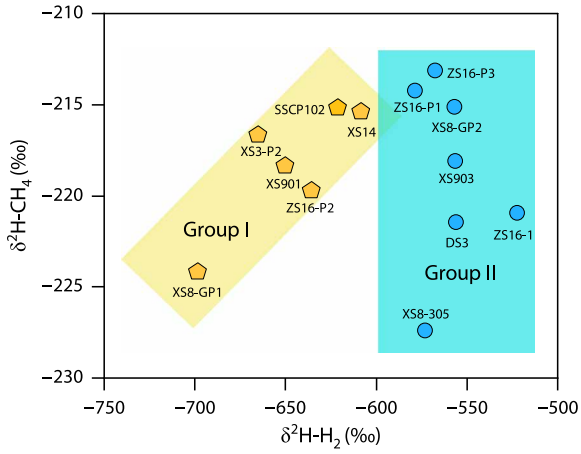

Fig. 3. Distribution characteristics of δ^2H-C_1 and δ^2H-H_2 values in Qingshen gas deposit, Songliao Basin. The distribution characteristics of the two groups of gases are shown: one with a positive correlation between δ^2H-C_1 and δ^2H-H_2 values, and another where δ^2H-H_2 values are greater, while δ^2H-C_1 values are more dispersed. The two group gases are automatically separated at a δ^2H-H_2 value of −600‰.

(*30*, *31*). The Qingshen gas deposit was calculated to have a mantle-derived helium contribution of 18.6%, based on a crust-mantle binary mixing model (fig. S2A) (*32*), indicating that mantle-derived volatile gases migrated and accumulated in the Qingshen gas deposit (*33*). Although there is no correlation between the R/Ra value and hydrogen concentration, possibly due to substantial consumption and conversion of hydrogen (fig. S2B), the geological conditions of the study area still support the accumulation of mantle-derived gases in shallow gas deposits.

DISCUSSION

Origin of natural hydrogen

More than 30 pathways for the natural hydrogen origin have been identified, which can be broadly categorized into organic and inorganic origins (*11*). Organic hydrogen may be derived from the thermal evolution of sedimentary organic matter and microbial activity. The inorganic genesis of hydrogen primarily includes water-rock interactions (WRI), water radiolysis, and deep-seated (hydrogen from the Earth's mantle or core) (*3*).

Hydrogen isotope fractionation can reveal geochemical and biochemical processes occurring on Earth (*34*). To some extent, δ^2H-H_2 can indicate the origin of natural hydrogen (*13*, *35*). We compiled 148 δ^2H-H_2 data points from around the world, representing various origins of natural hydrogen (fig. S3). The δ^2H-H_2 distribution range for WRI is broad, spanning −836 to −605‰. The average δ^2H-H_2 for water radiolysis is approximately −689‰. In the study on the origin of hydrogen in the Kansas Basin, USA, Liu *et al.* (*12*) pointed out that the δ^2H-H_2 values from WRI are lower than those from water radiolysis and that the hydrogen content associated with WRI is relatively higher. In contrast, δ^2H values of mantle-derived hydrogen are significantly greater, ranging between −665 and −332‰. Organic sources and biogenic δ^2H-H_2 are generally lighter, ranging from −810 to −629‰ and −828 to −699‰, respectively. Mantle-derived δ^2H-H_2 values are notably greater than hydrogen from crustal sources, as suggested in (*13*). The wide range of δ^2H-H_2 values obtained in this study, with overlaps among different origins (excluding biogenesis), suggests complex origins for the natural hydrogen. Because the temperature of the Qingshen gas deposit exceeds the upper thermal barrier for life (80° to 120°C) (*36*, *37*) and the δ^2H-H_2 values scarcely intersect with those typical of microbial genesis, it is reasonable to dismiss biogenesis as a source of hydrogen.

The equilibrium temperatures of hydrogen isotope fractionation and the kinetics of hydrogen exchange between H_2 and H_2O (D-H) (kinetic isotope effects) offer additional explanations for the variations in δ^2H-H_2 (*38*, *39*). The hydrogen isotope thermometer provides insights into the thermal history and conditions under which geological processes occur, particularly involving H_2O and hydrogen-containing minerals. The fractionation coefficient at hydrogen isotope equilibrium is highly sensitive to temperature (*40*). Proskurowski *et al.* (*41*) evaluated hydrogen isotope measurements of H_2, CH_4, and H_2O to identify the equilibrium fractionation factor, Δ, using the standard convention

$$\Delta_{A-B} = 1000\ln\alpha_{A-B} \quad (1)$$

where $\alpha_{A\text{-}B} = R_A/R_B$, for any isotope ratio R ($^{13}C/^{12}C$, D/H, etc.). It should be noted that defined this way, a positive Δ_{A-B} value indicates species B is isotopically depleted with respect to species A.

The hydrogen isotope equilibrium temperature for group I gases is relatively low, ranging from 61°C to 139°C, with an average of 105°C (Fig. 4). Conversely, the equilibrium temperature for group II gases is relatively high, ranging from 168° to 235°C, with an average of 192°C (Fig. 4). The average temperature of the Yingcheng Formation is approximately 140°C (fig. S4). Comparatively, the equilibrium temperature of group I gases is lower than the reservoir temperature, while the equilibrium temperature of group II gases is higher. This discrepancy suggests that the two groups of natural hydrogen are generated through different mechanisms at varying geological environments (temperatures or depths).

The hydrogen concentration and δ^2H-H_2 values of group I gases show a strong correlation (Fig. 5). As hydrogen concentration increases, δ^2H-H_2 values decrease. In addition, the equilibrium

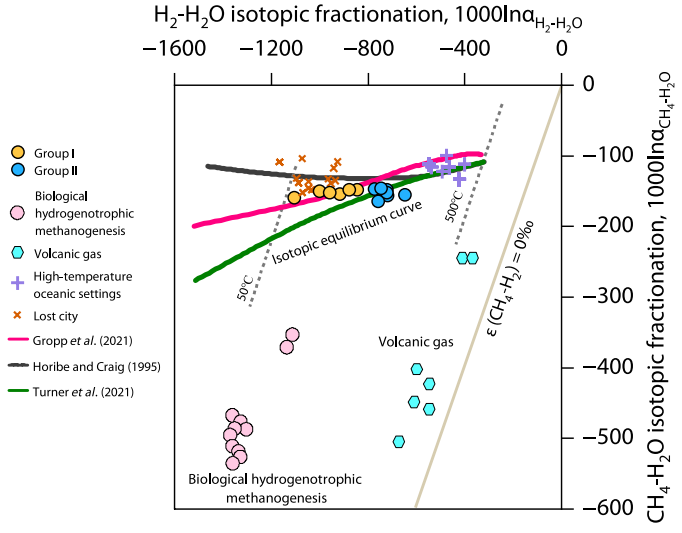

Fig. 4. CH_4-H_2-H_2O hydrogen isotope systematics: correlation between observed $1000\ln\alpha_{H_2-H_2O}$ and $1000\ln\alpha_{CH_4-H_2O}$ values. Hydrogen isotopic fractionation diagram modified from (*77*, *78*).

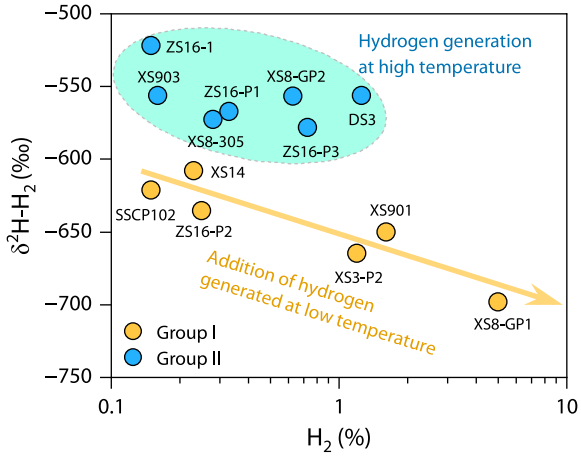

Fig. 5. Correlation of hydrogen concentration with δ^2H-H_2 values for the Qingshen gas deposit, Songliao Basin.

temperature of hydrogen isotopes in group I gases is relatively low, indicating that this group of hydrogen may primarily be associated with generation mechanisms under low-temperature conditions within sedimentary basins, such as WRI and water radiolysis. The gradual charging of hydrogen with lower isotope values, generated under low-temperature conditions, into natural gas reservoirs results in a negative correlation between hydrogen concentration and δ^2H-H_2 values. The extensive distribution of volcanic rocks (e.g., olivine basalts) and mafic-ultramafic intrusions in the study area provides conditions for WRI under low temperatures (*42*). Furthermore, two high-radiation sedimentary layers were identified in the SK2 well at depths of 3096.8 to 3102.8 m and 3168.3 to 3170.0 m, with U contents ranging from 5.9 to 29.3 ppm, Th contents from 5.5 to 37.3 ppm, and K contents from 2.9 to 4.3% (*43*, *44*). Natural hydrogen generated by water radiolysis could also migrate into natural gas reservoirs.

The high-temperature environment indicated by hydrogen isotopes in group II gases aligns with the basement temperature. The SK2 well encountered high hydrogen concentrations in the basement, with an average content of 18.60%, which is significantly higher than the levels found within the basin. Under the microscope, it was found that most of the rock slices of the basement were affected by WRI (hydrothermal alteration), and Fe(II)-containing minerals (such as pyroxene and amphibole) were once developed (*43*). The hydrogen production rates during alteration of peralkaline granites at 280° to 400°C are comparable and even faster than those documented for serpentinization of olivine and harzburgite (*45*). The hydrothermal alteration of pyroxene and amphibole in the basement rocks may be the main factor for the increase of its hydrogen content, which shows part of the crustal origin.

A review of natural hydrogen by Zgonnik (*11*) summarized some direct and indirect arguments for a deep-seated origin for hydrogen, including the superdeep drilling project, metal inclusions, first natural hydride (VH_2), and the association of hydrogen with fault zones. WRI involving mafic and ultramafic rocks in the upper mantle, the serpentinization of peridotite in subducting slabs, and primordial hydrogen support the generation of mantle-derived hydrogen (*11*, *46*–*48*). Mechanisms such as magmatic activity, mantle plumes, and deep fault channels transport mantle volatiles to the Earth's shallow crust (*49*, *50*). Volcanic-bearing sedimentary basins, such as the Songliao Basin, located at the leading edge of a subducting plate, exhibit frequent deep fluid activity, indicating that mantle-derived hydrogen may also be one of the hydrogen sources. The magmatic gases from the Satsuma-Iwojima volcano in the eastern Pacific, characterized by typical mantle signatures (R/Ra = 7.7, $CO_2/^3He = 8.16 \times 10^8$, $\delta^{13}C$-$CO_2 = -5.3‰$), allow us to use the $H_2/^3He$ value (9.71×10^8) from these volatiles to identify mantle-derived hydrogen (*51*). The $H_2/^3He$-R/Ra relationship diagram can distinguish between mantle-derived hydrogen and crustal-derived hydrogen (fig. S5) (*43*, *52*, *53*). Group II gases have an average R/Ra of 1.70 and an $H_2/^3He$ ratio of 1.87×10^7, while group I gases have an average R/Ra of 1.45 and an $H_2/^3He$ ratio of 2.96×10^7, indicating that both group I and group II gases are generally influenced by mantle-derived hydrogen, with group II gases containing a higher proportion of mantle-derived hydrogen. In addition, the Songliao Basin is located in a zone of multiple plate subductions and convergences, where notable lithospheric thinning and asthenospheric upwelling facilitate the entry of mantle-derived volatile gases (CO_2, H_2, He, etc.) into the basin (fig. S6) (*54*). The wells producing group II gases are closer to the Xuzhong deep fault compared to those producing group I gases, suggesting that mantle-derived volatiles containing hydrogen have migrated along the fault into the gas reservoirs. Figure S7 shows that high CO_2 concentrations and a portion of helium (mean, 18.6%) originate from the mantle, demonstrating that deep fluid activity facilitates the accumulation of various abiogenic gases in the shallow sedimentary basin. Therefore, it is speculated that group II gases are related to the process in which hydrogen, generated by hydrothermal alteration of basement rocks under high-temperature conditions and from the mantle, migrates through deep faults to the Yingcheng Formation.

Horsfield *et al.* (*55*) described the generation process of organic molecular hydrogen in the Songliao Basin (fig. S8). However, the temperature and maturity criteria for hydrocarbon source rocks to generate hydrogen are high, and only some areas' source rocks (Shahezi Formation) meet these conditions (fig. S9). Moreover, hydrogen generated during the maturation of kerogen is likely consumed by the aforementioned hydrogenation reactions. This is supported by the low hydrogen yields from pyrolysis of source rocks in both open and closed systems (*56*). It should be noted that we do not exclude the presence of organic hydrogen, as reported in (*55*), but the proportion of organic hydrogen in natural gas reservoirs may not be substantial.

Under experimental conditions, it was found that water directly participates in the generation of natural gas (*57*). Formation water engages in both low-temperature WRI and hydrogen exchange with hydrocarbon source rocks, thereby affecting the δ^2H values of both hydrogen and alkane gases. This explains the positive correlation exhibited by the group I gases in Fig. 3. The hydrogen in the group II gases primarily originates from high-temperature WRI occurring in basement rocks and from the mantle. Since the water in the basement does not interact with hydrocarbon source rocks, no correlation is observed between the δ^2H values of CH_4 and hydrogen in the group II gases in Fig. 3.

Here, we have established a crust-mantle mixed origin system for natural hydrogen in the volcanic-bearing sedimentary basin (Fig. 6). Specifically, natural hydrogen of the Qingshen gas deposit originates from low-temperature WRI in iron-rich rocks and water radiolysis of radioactive elements of source rocks within the basin, high-temperature WRI (hydrothermal alteration) and water radiolysis in

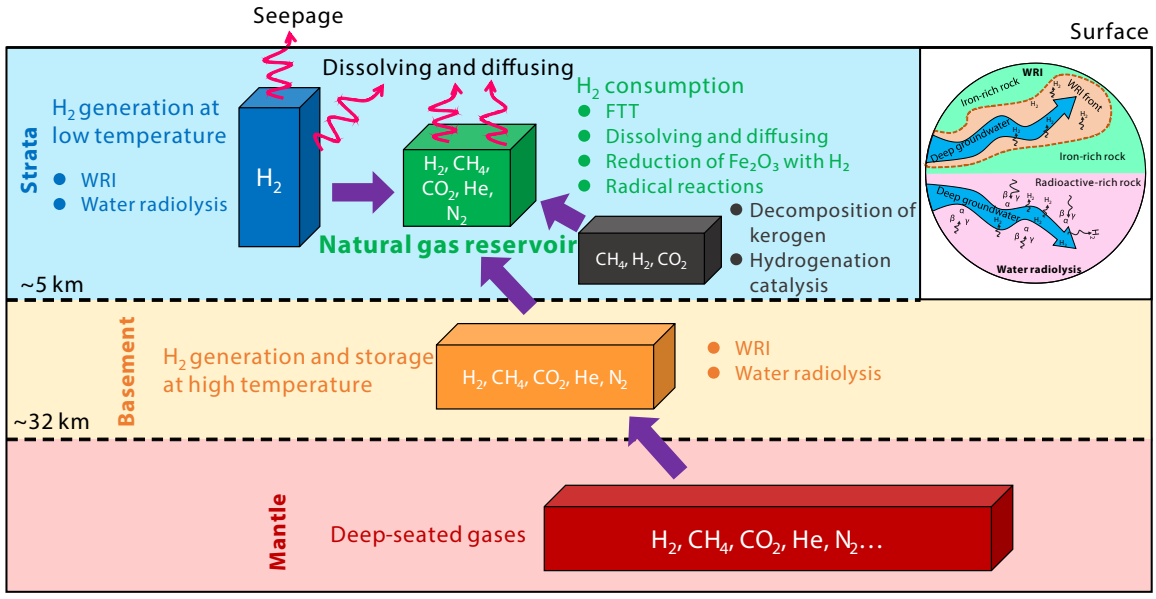

Fig. 6. The crust-mantle mixed origin system of natural hydrogen in the volcanic-bearing sedimentary basin.

basement rocks, as well as deep-seated hydrogen. Hydrogen in natural gas reservoirs may be consumed through Fischer-Tropsch–type (FTT) reactions, dissolution, diffusion, reduction of iron-containing minerals (*58*), and radical reactions between hydrogen and heavier gaseous hydrocarbons (*59*).

Conversion and original resource of natural hydrogen

The origin of alkane gases, especially in the Qingshen gas deposit of the Songliao Basin, has always been a controversial issue. The presence of heavier $\delta^{13}C_1$ values and the inverse feature in alkane carbon isotopes have been suggested as indicators of abiotic origins of alkane gases (*60*). According to Whiticar's carbon and hydrogen isotope scheme for the identification of the origin of CH_4 (*28*), the isotope values for the Qingshen gas deposit indicate that CH_4 formed under geothermal, hydrothermal, and crystalline conditions (fig. S10). In areas like the Songliao Basin, where there is deep fluid activity and faulted basins contain certain concentrations of hydrogen and mantle-derived CO_2, we must consider the contribution of abiotic CH_4 to natural gas reservoirs, including FTT reactions and mantle-derived CH_4 (*19*, *61*–*63*).

Figure 7A shows that as R/Ra increases, $\delta^{13}C_1$ tends to become greater, indicating the presence of mantle-derived abiotic CH_4. As hydrogen content decreases, $\delta^{13}C_1$ increases (Fig. 7B), suggesting increased abiotic gas components. This change reflects the FTT reactions, where hydrogen reacts with CO_2 to form abiotic CH_4. When residual CO_2 content is high, the $\delta^{13}C_1$ and $\delta^{13}C_2$ typically exhibit reversal (Fig. 7C), indicating that the FTT reactions partially consume a large amount of mantle-derived CO_2 until hydrogen content is insufficient to sustain it, leaving excess CO_2. Conversely, samples with low CO_2 content may not be influenced by mantle degassing, resulting in an insufficient carbon source for the FTT reactions, and thus no reversal in alkane carbon isotopes. R/Ra, $CO_2/^3He$, and $CH_4/^3He$ ratios are used to infer the possible crustal or mantle origins of gases (*64*). Almost all samples fall into the lower part of the magmatic range, and relative to ^3He, they appear to have experienced CO_2 loss and dissolution (fig. S11A). As shown in fig. S11B, most of the gas samples from the Songliao Basin are above the two-component mixing area between crustal and mantle endmembers, suggesting that additional CH_4 input has resulted in high $CH_4/^3He$ values in gas samples associated with high R/Ra ratios. The $CH_4/^3He$ values in the other group gases, where δ^2H-H_2 could not be measured due to low hydrogen concentrations, are higher than in groups I and II. This reveals that a substantial amount of hydrogen has been consumed and converted into additional CH_4. The loss of CO_2 and the anomalously high levels of CH_4 are indicative of the FTT reactions.

The geological setting characterized by deep fluid activity facilitates the conversion of hydrogen from various origins and mantle-derived CO_2 into CH_4, yielding $\delta^{13}C_1$ signatures (*65*). The efficiency of FTT reactions is contingent on both the presence of catalysts and specific thermal conditions. Iron, nickel, cobalt, chromium, and minerals containing these metals are recognized catalysts in FTT reactions, enabling the reaction to occur naturally within geological formations even under conditions of low temperature and pressure, albeit over extended periods (*18*, *63*). For example, natural gas from serpentinized peridotites in Chimaera, containing chromite, with 9.76% H_2 and 85.7% CH_4, is believed to have been generated through low-temperature (<50°C) FTT methanation (*6*). The Yingcheng Formation and the basin's basement, both rich in iron-containing mafic rocks, are potential sites for the FTT reactions to produce abiotic CH_4. This CH_4 then migrates and mixes with organically derived gases to form natural gas reservoirs.

The linear mixing model proposed in (*64*) was used to estimate the CH_4 content from different origins (Supplementary Materials). The results show that the proportion of abiotic CH_4 in the Qingshen gas deposit ranges from 24.99 to 49.26% (excluding wells DS3 and DS17), with an average of 37.75%. This result is consistent with the distribution characteristics of $\delta^{13}C$ values of the Qingshen gas deposit on the mixing lines between thermogenic and abiotic endmembers established in (*6*) (fig. S12). By 2018, the proven natural gas reserves of the Qingshen gas deposit had reached 252.271×10^9 m^3 (*64*). On

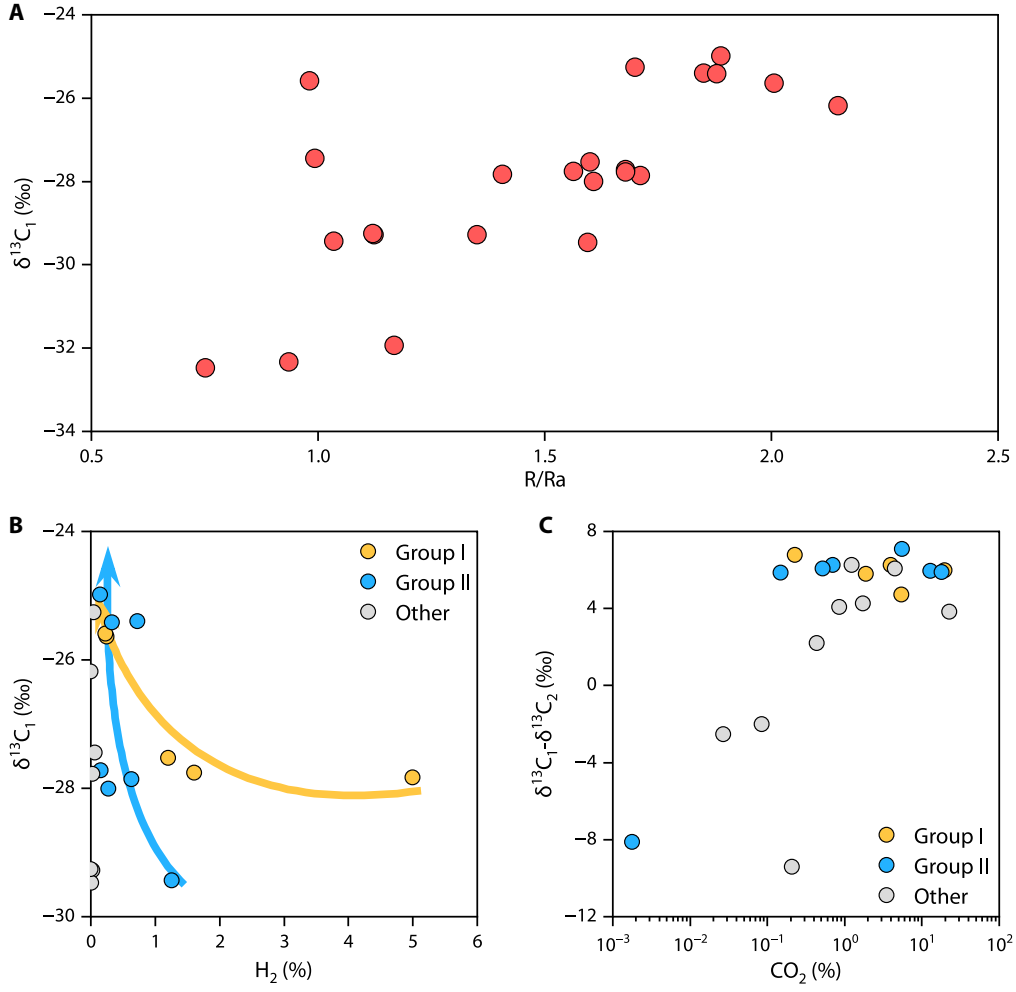

Fig. 7. Contribution of abiotic CH_4 to natural gas reservoirs. (**A**) There is a positive correlation between R/Ra and $\delta^{13}C_1$ values. (**B**) As hydrogen content decreases, $\delta^{13}C_1$ values become greater. (**C**) Relationship between CO_2 content and $\delta^{13}C_1$-$\delta^{13}C_2$ values.

the basis of previous calculations, it is estimated that the Qingshen gas deposit contains approximately 95.23×10^9 m^3 of abiotic CH_4. Therefore, the abiotic alkane gas in the Qingshen gas deposit has promising exploration prospects. Abiotic alkane gas can form commercial accumulations under specific geological conditions, which holds positive and practical significance for expanding natural gas exploration in sedimentary basins.

A mixing model using crust-mantle endmembers (with $\delta^{13}C_1$ values set at −30.0 and −15.0‰, respectively) calculates that the proportions of mantle-derived and FTT CH_4 in natural gas are 31.70 and 6.04%, respectively. Approximately 15.24×10^9 m^3 of CH_4 is estimated to be derived from FTT reactions. The FTT reactions between H_2 and CO_2, which produce 1 mol of CH_4, require the consumption of 4 mol of H_2 and 1 mol of CO_2. Using the gas conversion ratios from the FTT reactions, we estimated the proportion of CO_2 and H_2 involved in the conversion. The FTT reactions consumed up to 15.24×10^9 m^3 of mantle-derived CO_2. Using the average CO_2 content of 4.4% in the Qingshen gas deposit, the current CO_2 reserves are calculated to be around 3.79×10^9 m^3. This indicates that at least 19.03×10^9 m^3 of mantle-derived CO_2 was released into the shallow crust. After accounting for the conversion, we calculated the maximum original hydrogen concentrations in the gas reservoir range from 13.79 to 24.08%, with an average of 19.80% (Fig. 8). Further estimates suggest that the maximum original hydrogen reserves in the Qingshen gas deposit are 61.9×10^9 m^3. Here, we state that the calculated original hydrogen contents are overestimated (representing the maximum original hydrogen content), as FTT reactions also occurs outside the reservoir (e.g., in the basin basement), where the natural hydrogen within the reservoir is not consumed.

With an average hydrogen concentration of 0.53% in the collected gas samples, the current hydrogen reserves in the Qingshen gas deposit are estimated to be 1.34×10^9 m^3. The results indicate that approximately 97.8% of hydrogen has been consumed through conversion. Natural gas systems in volcanic-bearing sedimentary basins can serve as sites for the accumulation of large amounts of natural hydrogen. However, hydrogen from different origins is often substantially consumed, leading to generally low hydrogen concentrations in current natural gas reservoirs.

Production rates of natural hydrogen

Overall, natural hydrogen in the Songliao Basin primarily originates from water radiolysis, WRI, and mantle. Cheng *et al.* (*66*) investigated

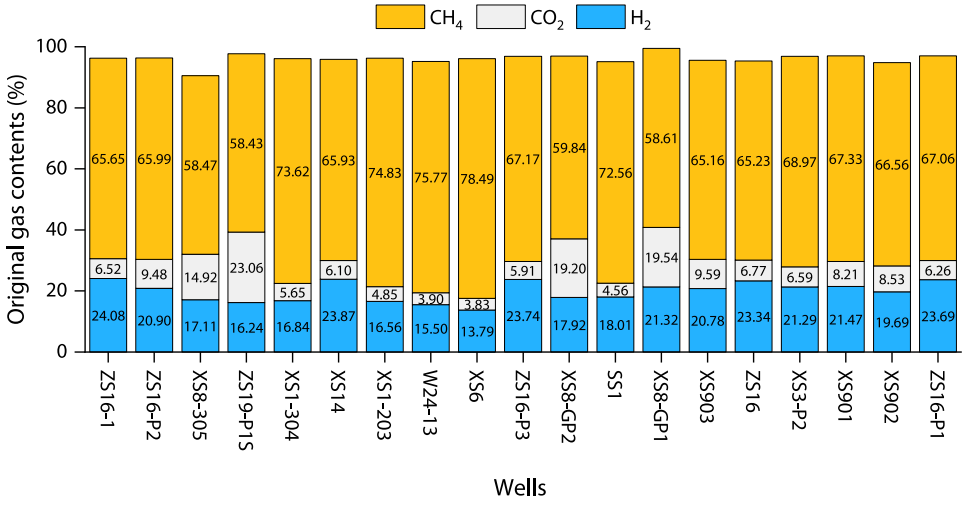

Fig. 8. Maximum original gas contents in the Qingshen gas deposit.

the proportion of gas loss due to dissolution and diffusion during the migration of degassed gases from the deep crust to the overlying strata. In contrast, this paper primarily assesses the natural gas system's capacity to trap hydrogen from different origins. We assume that natural gas reservoirs can only store hydrogen generated beneath them. In addition, we developed a geological model of the source-reservoir combination for natural hydrogen in the volcanic-bearing sedimentary basins to facilitate the calculation of hydrogen store rates. This model includes several layers, ranging from shallow to deep: natural gas reservoirs (traps), strata (extending from the natural gas reservoirs to the top of the basement), part of the upper crust (from the top of the basement to the top of the middle crust), the middle crust, the lower crust, and the mantle (mantle-derived hydrogen). We did not consider the influence of hydrogen generation in the middle and lower crust, as their water-filled porosity may be insufficient to support hydrogen production. The basic geological parameters of this model can be found in the Supplementary Materials.

The natural emission of α, β, and γ particles resulting from the decay of uranium (U), thorium (Th), and potassium (K) was assessed in (*67*, *68*) for typical granite, basalt, and quartzite lithologies. This assessment served as the foundation for calculating radiolytic hydrogen production. In the radiolytic hydrogen model, Sherwood Lollar *et al.* (*5*) derived a crust fracture porosity related radiolytic hydrogen rate of 16×10^9 mol H_2 $year^{-1}$(358.0 MMm^3/year at standard temperature and pressure) for global Precambrian continental lithosphere. On the basis of the genetic method in (*5*, *14*), we calculated a maximum radiolytic hydrogen production rate of 286.0 MMm^3/year and a ^{4}He production rate of 5.9 MMm^3/year in the Songliao Basin. The earliest time of natural gas accumulation is approximately 100 Ma (*69*), which may also be when natural hydrogen began to be trapped. The Songliao Basin has generated a maximum total of 28.6×10^{12} m^3 of radiolytic hydrogen over this time. Further calculations indicate that the crust below the Qingshen gas deposit in the Xujiaweizi Depression has generated up to 572×10^9 m^3 of radiolytic hydrogen.

Several studies have provided estimates of global hydrogen production from marine systems, including both volcanic/magmatic sources and hydrogen production from the abiogenic WRI that are the focus of this paper (*5*). Water radiolysis based on radioelement concentration and porosity is tied to ^{4}He production, and mineral hydration dominantly associated with rock type and independent of noble gas production (*22*). Most studies follow the approach typical for the marine literature, using reaction-based models with a governing equation relating oxidation of FeO in the crust to hydrogen production at a ratio of 3:1 that is either of the form of equation 2 of (*70*).

$$3FeO\ (\text{in silicates}) + H_2O \rightarrow Fe_3O_4\ (\text{magnetite}) + H_2 \qquad (2)$$

In our study, we used the numerical method of Sherwood Lollar *et al.* (*5*) to quantify the hydrogen produced through WRI. Briefly, the 2014 model estimated that every 1 m^3 of near-surface mafic and ultramafic rock had the potential to produce up to 1400 mol of H_2 through WRI. If the efficiency of WRI reaches 100%, the calculations indicate that WRI in rocks from the depth of the Qingshen gas deposit in the Songliao Basin (3 km) to the bottom of the upper crust (12.75 km) has produced a total of 1.16×10^{18} mol of H_2. On the basis of the age of the strata [113 Ma; (*71*)] and basement rocks [954 Ma; (*72*)], a hydrogen production rate of 5.53×10^9 mol/year from WRI was estimated, equivalent to 124.0 MMm^3 H_2 $year^{-1}$. The cumulative maximum production of WRI hydrogen in the Xujiaweizi Depression since 100 Ma was calculated to be 248×10^9 m^3.

The flux of mantle-derived hydrogen in natural gas reservoirs was estimated using mantle-derived hydrogen and helium from the magmatic volatiles of the Satsuma-Iwojima volcano in the eastern Pacific. According to (*51*), the maximum $H_2/^3$He value in these volatiles is approximately 9.71×10^8. The average ^{3}He content in the Qingshen gas deposit is 5.19×10^{-8}. Using the maximum $H_2/^3$He value from the Satsuma-Iwojima volcano, the maximum total production of mantle-derived hydrogen is estimated to account for 50% of the Qingshen gas deposit's reserves, amounting to approximately 127×10^9 m^3.

On the basis of the hydrogen production rates from radiolysis, WRI, and mantle sources, a maximum total of 947×10^9 m^3 of natural hydrogen has been generated in the lower part of the Qingshen gas deposit. The hydrogen store rate of the restored natural gas system

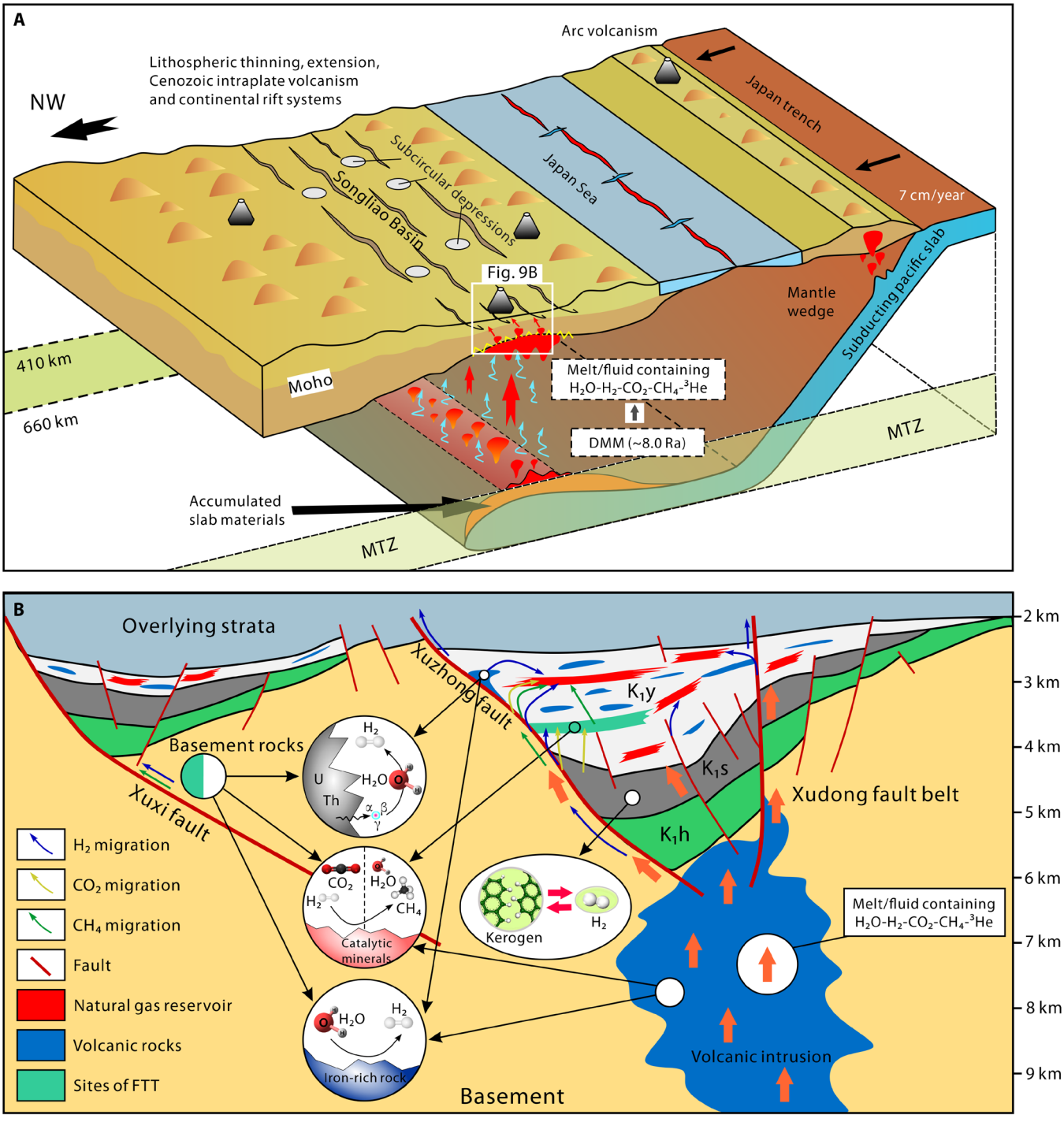

Fig. 9. The formation model of natural hydrogen in the Songliao Basin. (**A**) Under the subduction of the Paleo-Pacific Plate, deep fluids carrying volatiles traverse lithospheric layers into the shallow crust and release gases, modified from (*79*). NW, northwest; MTZ, mantle transition zone; DMM, depleted upper mantle. (**B**) Sedimentary basins and basement rocks generate and consume hydrogen through WRI, water radiolysis, decomposition of organic matter, and FTT reactions. The geological structural framework of the basin is modified from (*80*), and the kerogen structure is sourced from (*81*).

is 6.6%, while the current natural gas system (after consumption and conversion) has a hydrogen store rate of 1.4% (table S2). These data indicate that the hydrogen store rate of natural gas systems can be considerable, particularly in volcanic-bearing sedimentary basins. Given the favorable geological conditions for trapping natural hydrogen and the substantial gas reserves in natural gas deposits, the hydrogen within natural gas systems deserves considerable attention.

The formation model of natural hydrogen in the Songliao Basin

Unlike other geological structures, the formation process of hydrogen-rich natural gas reservoirs in volcanic-bearing sedimentary basins is more complex. This process is analogous to the generation of oil and gas from source rocks and their subsequent migration to traps for accumulation. However, it often involves multiple hydrogen-generating geological processes and interactions between different spheres of the Earth.

In the Songliao Basin, there is intense interaction between the shallow crust and the deep mantle. Deep fluids, as important carriers of materials and energy from the Earth's interior, facilitate the transfer of matter and energy across Earth's spheres through major structural channels. This phenomenon is common in active tectonic zones such as continental rift basins and mid-ocean ridges. Volatile gases from the mantle, as essential components of Earth's deep fluids, accompany magmatic effusion and intrusion activities during mantle degassing. These gases mainly include CO_2, H_2O, SO_2, H_2S, N_2, CH_4, H_2, and rare gases (*73*, *74*). Upwelling of asthenospheric material beneath the Songliao Basin, along with partial melting and thinning of the crust, reduces the stress exerted by the overlying rocks, creating favorable conditions for the ascent of deep fluids. Deep fluids carrying mantle-derived volatile gases disperse upward along trans-crustal faults and are trapped by geological bodies capable of storing hydrogen, forming natural hydrogen gas accumulations (Fig. 9A).

The basement of the Songliao Basin is a notable site for hydrogen generation. WRI (iron-rich rocks and water), radiolytic decomposition of water, and injection of mantle-derived volatiles are reasons for the high concentrations of hydrogen in the basement. Natural hydrogen in the basement can migrate through fault systems into the Songliao Basin and be stored by hydrogen-storing geological bodies, forming hydrogen gas accumulations (Fig. 9B) (*50*). The sedimentary strata of the Songliao Basin also have the capacity to generate hydrogen. Organic matter in the Shahezi Formation, under high temperatures and a high degree of thermal evolution, produces organically natural hydrogen (*55*), which may then enter natural gas reservoirs through oil and gas migration pathways. The mafic intrusive rock bodies within the basin can generate hydrogen through WRI at low temperatures. In addition, the decay of radioactive elements in volcanic rocks can decompose water to produce hydrogen. Besides diffusion loss, the FTT reaction occurring in the basement and sedimentary strata is another important mechanism for hydrogen loss. Mixing of varying concentrations of abiotic and biotic CH_4 may occur in the deep natural gas reservoirs of the Songliao Basin.

MATERIALS AND METHODS

Sampling

Natural gas was meticulously collected from the Yingcheng Formation of the Qingshen gas deposit across 23 wells within the Xujiahuizi fault depression, Songliao Basin. The collected gas samples were ensured to be pure by directly extracting them from wellheads within operational hydrocarbon deposits. A preliminary step involved purging the lines for a duration of 15 to 20 min, a process aimed at eliminating any potential air impurities, thereby ensuring the integrity of the samples for subsequent analysis. We used a robust stainless steel cylinder, precisely 25 cm in diameter and capable of holding about 10 liters of gas. These cylinders were fitted with dual shut-off valves designed to withstand up to 22.5 MPa. The protocol required maintaining internal pressure above 5.0 MPa to avoid air contamination, with a thorough water immersion leak test following sample collection.

Natural gas composition analysis

Analyses for determining the relative molecular composition of the gases were performed by gas chromatograph in the laboratory of the Oil and Gas Resources Research Center, Northwest Institute of Eco-Environment and Resources, Chinese Academy of Sciences. Hydrocarbon gases were analyzed on a GC5890N equipped with a flame ionization detector and an Al_2O_3 column (30 m by 0.53 mm), with N_2 as the carrier gas. The oven temperature program for the Al_2O_3 column was set to 0°C for 3 min, followed by heating at 10°C/min to 180°C (5 min hold). Nonhydrocarbon gases (such as H_2, N_2, and He) were analyzed using a GC9790 equipped with a thermal conductivity detector and a TDX-01 column (3 m by 3 mm). The oven temperature program for the TDX-01 column started at 40°C for 5 min, followed by heating at 10°C/min to 240°C (10-min hold).

Isotope analysis

Stable carbon isotope compositions were accurately measured using a Finnigan MAT-253 instrument. This detailed gas chromatographic analysis involved a Porapak Q column and carefully controlled temperature settings to progressively increase from 40° to 160°C. Pure helium was used as the carrier gas at a flow rate of 1.2 ml/min, with the analytical precision for $\delta^{13}C$ values maintained within <0.3‰. Each sample was measured three times, and the results of the three measurements were averaged. δ^2H measurements were conducted on a Deltaplus XP mass spectrometer under finely tuned gas chromatography conditions, ensuring the precision of δ^2H values to within 3.0‰, Vienna standard mean ocean water. The minimum hydrogen concentration for δ^2H measurements is 0.1%. Each sample was measured three times, and the results of the three measurements were averaged. The $^3He/^4He$ ratios were determined with a Noblesse noble gas mass spectrometer (Nu Instruments, UK) calibrated with air from the Gaolan Hill area south of Lanzhou.

Supplementary Materials

This PDF file includes:

Supplementary Text
Figs. S1 to S12
Tables S1 and S2
References

REFERENCES AND NOTES

1. IEA, "The Future of Hydrogen" (2019); https://iea.org/reports/the-future-of-hydrogen.
2. M. Liebreich, "The Clean Hydrogen Ladder [Now updated to V4.1]" (Liebreich Associates, 2021); https://liebreich.com/the-clean-hydrogen-ladder-now-updated-to-v4-1/.
3. E. Hand, Hidden hydrogen: Earth may hold vast stores of a renewable, carbon-free fuel? *Science* **379**, 630–636 (2023).
4. F. Osselin, C. Soulaine, C. Fauguerolles, E. C. Gaucher, B. Scaillet, M. Pichavant, Orange hydrogen is the new green. *Nat. Geosci.* **15**, 765–769 (2022).

5. B. Sherwood Lollar, T. C. Onstott, G. Lacrampe-Couloume, C. J. Ballentine, The contribution of the Precambrian continental lithosphere to global H_2 production. *Nature* **516**, 379–382 (2014).
6. G. Etiope, M. Schoell, H. Hosgörmez, Abiotic methane flux from the Chimaera seep and Tekirova ophiolites (Turkey): Understanding gas exhalation from low temperature serpentinization and implications for Mars. *Earth Planet. Sci. Lett.* **310**, 96–104 (2011).
7. J. Guélard, V. Beaumont, V. Rouchon, F. Guyot, D. Pillot, D. Jézéquel, M. Ader, K. D. Newell, E. Deville, Natural H_2 in Kansas: Deep or shallow origin? *Geochem. Geophys. Geosyst.* **18**, 1841–1865 (2017).
8. C. Neal, G. Stanger, Hydrogen generation from mantle source rocks in Oman. *Earth Planet. Sci. Lett.* **66**, 315–320 (1983).
9. L. Truche, F.-V. Donzé, E. Goskolli, B. Muceku, C. Loisy, C. Monnin, H. Dutoit, A. Cerepi, A deep reservoir for hydrogen drives intense degassing in the Bulqizë ophiolite. *Science* **383**, 618–621 (2024).
10. C. Vacquand, E. Deville, V. Beaumont, F. Guyot, O. Sissmann, D. Pillot, C. Arcilla, A. Prinzhofer, Reduced gas seepages in ophiolitic complexes: Evidences for multiple origins of the H_2-CH_4-N_2 gas mixtures. *Geochim. Cosmochim. Acta* **223**, 437–461 (2018).
11. V. Zgonnik, The occurrence and geoscience of natural hydrogen: A comprehensive review. *Earth Sci. Rev.* **203**, 103140 (2020).
12. Q. Liu, X. Wu, Q. Meng, D. Zhu, X. Huang, D. Zhu, P. Li, Z. Jin, Natural hydrogen: A potential carbon-free energy source. *Chin. Sci. Bull.* **69**, 2344–2350 (2024).
13. A. V. Milkov, Molecular hydrogen in surface and subsurface natural gases: Abundance, origins and ideas for deliberate exploration. *Earth Sci. Rev.* **230**, 104063 (2022).
14. C. J. Boreham, D. S. Edwards, K. Czado, N. Rollet, L. Wang, S. van der Wielen, D. Champion, R. Blewett, A. Feitz, P. A. Henson, Hydrogen in Australian natural gas: Occurrences, sources and resources. *APPEA J.* **61**, 163–191 (2021).
15. O. Jackson, S. R. Lawrence, I. P. Hutchinson, A. E. Stocks, A. C. Barnicoat, M. Powney, Natural hydrogen: Sources, systems and exploration plays. *Geoenergy* **2**, geoenergy2024–2002 (2024).
16. O. Maiga, E. Deville, J. Laval, A. Prinzhofer, A. B. Diallo, Trapping processes of large volumes of natural hydrogen in the subsurface: The emblematic case of the Bourakebougou H_2 field in Mali. *Int. J. Hydrogen Energy* **50**, 640–647 (2024).
17. A. Prinzhofer, C. S. Tahara Cissé, A. B. Diallo, Discovery of a large accumulation of natural hydrogen in Bourakebougou (Mali). *Int. J. Hydrogen Energy* **43**, 19315–19326 (2018).
18. G. Etiope, M. J. Whiticar, Abiotic methane in continental ultramafic rock systems: Towards a genetic model. *Appl. Geochem.* **102**, 139–152 (2019).
19. G. Proskurowski, M. D. Lilley, J. S. Seewald, G. L. Früh-Green, E. J. Olson, J. E. Lupton, S. P. Sylva, D. S. Kelley, Abiogenic hydrocarbon production at lost city hydrothermal field. *Science* **319**, 604–607 (2008).
20. Q. Williams, R. J. Hemley, Hydrogen in the deep Earth. *Annu. Rev. Earth Planet. Sci.* **29**, 365–418 (2001).
21. R. Karolytė, O. Warr, E. van Heerden, S. Flude, F. de Lange, S. Webb, C. J. Ballentine, B. Sherwood Lollar, The role of porosity in H_2/He production ratios in fracture fluids from the Witwatersrand Basin, South Africa. *Chem. Geol.* **595**, 120788 (2022).
22. O. Warr, T. Giunta, C. J. Ballentine, B. Sherwood Lollar, Mechanisms and rates of ^{4}He, ^{40}Ar, and H_2 production and accumulation in fracture fluids in Precambrian Shield environments. *Chem. Geol.* **530**, 119322 (2019).
23. M. Feng, M. J. An, H. S. Hou, T. Y. Fan, H. L. Zang, Channelised magma ascent and lithospheric zonation beneath the Songliao Basin, Northeast China, based on surface-wave tomography. *Tectonophysics* **862**, 229969 (2023).
24. Z. Li, J. Chen, H. Zou, C. Wang, Q. Meng, H. Liu, S. Wang, Mesozoic–Cenozoic tectonic evolution and dynamics of the Songliao Basin, NE Asia: Implications for the closure of the Paleo-Asian Ocean and Mongol-Okhotsk Ocean and subduction of the Paleo-Pacific Ocean. *Earth Sci. Rev.* **218**, 103471 (2021).
25. S. Han, Z. Tang, C. Wang, B. Horsfield, T. Wang, N. Mahlstedt, Hydrogen-rich gas discovery in continental scientific drilling project of Songliao Basin, Northeast China: New insights into deep Earth exploration. *Sci. Bull.* **67**, 1003–1006 (2022).
26. M. Schoell, Genetic characterization of natural gases. *AAPG Bull.* **67**, 2225–2238 (1983).
27. Y. Zou, Y. Cai, C. Zhang, X. Zhang, P. Peng, Variations of natural gas carbon isotope-type curves and their interpretation – A case study. *Org. Geochem.* **38**, 1398–1415 (2007).
28. H. Wycherley, A. Fleet, H. Shaw, Some observations on the origins of large volumes of carbon dioxide accumulations in sedimentary basins. *Mar. Pet. Geol.* **16**, 489–494 (1999).
29. B. Sherwood Lollar, K. Voglesonger, L. H. Lin, G. Lacrampe-Couloume, J. Telling, T. A. Abrajano, T. C. Onstott, L. M. Pratt, Hydrogeologic controls on episodic H_2 release from precambrian fractured rocks—Energy for deep subsurface life on Earth and Mars. *Astrobiology* **7**, 971–986 (2007).
30. E. R. Oxburgh, R. K. O'Nions, R. I. Hill, Helium isotopes in sedimentary basins. *Nature* **324**, 632–635 (1986).
31. D. W. Graham, Noble gas isotope geochemistry of mid-ocean ridge and ocean island basalts: Characterization of mantle source reservoirs. *Rev. Mineral. Geochem.* **47**, 247–317 (2002).
32. C. J. Ballentine, R. K. O'Nions, The nature of mantle neon contributions to Vienna Basin hydrocarbon reservoirs. *Earth Planet. Sci. Lett.* **113**, 553–567 (1992).
33. Q. Liu, X. Wu, X. Wang, Z. Jin, D. Zhu, Q. Meng, S. Huang, J. Liu, Q. Fu, Carbon and hydrogen isotopes of methane, ethane, and propane: A review of genetic identification of natural gas. *Earth Sci. Rev.* **190**, 247–272 (2019).
34. F. Robert, S. Derenne, G. Lombardi, K. Hassouni, A. Michau, P. Reinhardt, R. Duhamel, A. Gonzalez, K. Biron, Hydrogen isotope fractionation in methane plasma. *Proc. Natl. Acad. Sci. U.S.A.* **114**, 870–874 (2017).
35. Q. Liu, X. Wu, X. Huang, D. Zhu, Q. Meng, D. Zhu, H. Xu, J. Liu, P. Li, Z. Zhou, K. Zhang, Z. Jin, Integrated geochemical identification of natural hydrogen sources. *Sci. Bull.* **24**, S2095–S9273 (2024).
36. F. Beulig, F. Schubert, R. R. Adhikari, C. Glombitza, V. B. Heuer, K. U. Hinrichs, K. L. Homola, F. Inagaki, B. B. Jørgensen, J. Kallmeyer, S. J. E. Krause, Y. Morono, J. Sauvage, A. J. Spivack, T. Treude, Rapid metabolism fosters microbial survival in the deep, hot subseafloor biosphere. *Nat. Commun.* **13**, 312 (2022).
37. I. M. Head, D. M. Jones, S. R. Larter, Biological activity in the deep subsurface and the origin of heavy oil. *Nature* **426**, 344–352 (2003).
38. N. J. Pester, M. E. Conrad, K. G. Knauss, D. J. DePaolo, Kinetics of D/H isotope fractionation between molecular hydrogen and water. *Geochim. Cosmochim. Acta* **242**, 191–212 (2018).
39. A. Ricci, B. I. Kleine, J. Fiebig, J. Gunnarsson-Robin, K. Mativo Kamunya, B. Mountain, A. Stefánsson, Equilibrium and kinetic controls on molecular hydrogen abundance and hydrogen isotope fractionation in hydrothermal fluids. *Earth Planet. Sci. Lett.* **579**, 117338 (2022).
40. Y. Horibe, H. Craig, DH fractionation in the system methane-hydrogen-water. *Geochim. Cosmochim. Acta* **59**, 5209–5217 (1995).
41. G. Proskurowski, M. D. Lilley, D. S. Kelley, E. J. Olson, Low temperature volatile production at the Lost City Hydrothermal Field, evidence from a hydrogen stable isotope geothermometer. *Chem. Geol.* **229**, 331–343 (2006).
42. C. Liu, E. Nicotra, X. Shan, J. Yi, G. Ventura, The Cretaceous volcanism of the Songliao Basin: Mantle sources, magma evolution processes and implications for the NE China geodynamics - A review. *Earth Sci. Rev.* **237**, 104294 (2023).
43. S. Han, C. Xiang, X. Du, L. Xie, J. Huang, C. Wang, Geochemistry and origins of hydrogen-containing natural gases in deep Songliao Basin, China: Insights from continental scientific drilling. *Pet. Sci.* **21**, 741–751 (2024).
44. G. Wang, W. Lin, F. Liu, H. Gan, S. Wang, G. Yue, X. Long, Y. Liu, Theory and survey practice of deep heat accumulation in geothermalsystem and exploration practice. *Acta Geol. Sin.* **97**, 639–660 (2023).
45. L. Truche, F. Bourdelle, S. Salvi, N. Lefeuvre, A. Zug, E. Lloret, Hydrogen generation during hydrothermal alteration of peralkaline granite. *Geochim. Cosmochim. Acta* **308**, 42–59 (2021).
46. J. R. Smyth, D. J. Frost, F. Nestola, C. M. Holl, G. Bromiley, Olivine hydration in the deep upper mantle: Effects of temperature and silica activity. *Geophys. Res. Lett.* **33**, L15301 (2006).
47. S. Demouchy, N. Bolfan-Casanova, Distribution and transport of hydrogen in the lithospheric mantle: A review. *Lithos* **240-243**, 402–425 (2016).
48. A. S. Merdith, I. Daniel, D. Sverjensky, M. Andreani, B. Mather, S. Williams, A. Vitale Brovarone, Global hydrogen production during high-pressure serpentinization of subducting slabs. *Geochem. Geophys. Geosyst.* **24**, e2023GC010947 (2023).
49. H. Liu, B. Zhang, H. Fei, L. Liu, A first-principles molecular dynamics study of molecular hydrogen diffusion in Fe-free olivine. *Geosci. Front.* **16**, 101926 (2025).
50. B. H. Lodhia, L. Peeters, E. Frery, A review of the migration of hydrogen from the planetary to basin scale. *J. Geophys. Res. Solid Earth* **129**, e2024JB028715 (2024).
51. T. P. Fischer, G. Chiodini, "Chapter 45 - Volcanic, magmatic and hydrothermal gases" in *The Encyclopedia of Volcanoes* (Second Edition), H. Sigurdsson, Ed. (Academic Press, 2015), pp. 779–797.
52. Z. Jin, W. Hu, L. Zhang, M. Tao, *Deep-derived Fluid and its Effect on Hydrocarbon Cccumulation* (Science Press, Beijing, 2007).
53. Q. Meng, Y. Sun, J. Tong, Q. Fu, J. Zhu, D. Zhu, Z. Jin, Distribution and geochemical characteristics of hydrogen in natural gas from the jiyang depression, Eastern China. *Acta Geol. Sin. (Engl. Ed.)* **89**, 1616–1624 (2015).
54. D. V. Bekaert, S. J. Turner, M. W. Broadley, J. D. Barnes, S. A. Halldórsson, J. Labidi, J. Wade, K. J. Walowski, P. H. Barry, Subduction-driven volatile recycling: A global mass balance. *Annu. Rev. Earth Planet. Sci.* **49**, 37–70 (2021).
55. B. Horsfield, N. Mahlstedt, P. Weniger, D. Misch, S. Vranjes-Wessely, S. Han, C. Wang, Molecular hydrogen from organic sources in the deep Songliao Basin, P.R. China. *Int. J. Hydrogen Energy* **47**, 16750–16774 (2022).
56. X. Li, J. Horita, Kinetic and equilibrium reactions on natural and laboratory generation of thermogenic gases from Type II marine shale. *Geochim. Cosmochim. Acta* **333**, 263–283 (2022).
57. A. Schimmelmann, M. D. Lewan, R. P. Wintsch, D/H isotope ratios of kerogen, bitumen, oil, and water in hydrous pyrolysis of source rocks containing kerogen types I, II, IIS, and III. *Geochim. Cosmochim. Acta* **63**, 3751–3766 (1999).

58. M. N. A. Tahari, F. Salleh, T. S. T. Saharuddin, A. Samsuri, S. Samidin, M. A. Yarmo, Influence of hydrogen and carbon monoxide on reduction behavior of iron oxide at high temperature: Effect on reduction gas concentrations. *Int. J. Hydrogen Energy* **46**, 24791–24805 (2021).
59. S. Lu, J. Li, H. Xue, F. Chen, Q. Xu, M. Wang, W. Li, X. Pang, Pyrolytic gaseous hydrocarbon generation and the kinetics of carbon isotope fractionation in representative model compounds with different chemical structures. *Geochem. Geophys. Geosyst.* **20**, 1773–1793 (2019).
60. B. Sherwood Lollar, T. D. Westgate, J. A. Ward, G. F. Slater, G. Lacrampe-Couloume, Abiogenic formation of alkanes in the Earth's crust as a minor source for global hydrocarbon reservoirs. *Nature* **416**, 522–524 (2002).
61. H. P. Scott, R. J. Hemley, H.-k. Mao, D. R. Herschbach, L. E. Fried, W. M. Howard, S. Bastea, Generation of methane in the Earth's mantle: In situ high pressure–temperature measurements of carbonate reduction. *Proc. Natl. Acad. Sci. U.S.A.* **101**, 14023–14026 (2004).
62. A. Kolesnikov, V. G. Kutcherov, A. F. Goncharov, Methane-derived hydrocarbons produced under upper-mantle conditions. *Nat. Geosci.* **2**, 566–570 (2009).
63. G. Etiope, B. Sherwood Lollar, Abiotic methane on Earth. *Rev. Geophys.* **51**, 276–299 (2013).
64. Q. Liu, J. Dai, Z. Jin, J. Li, X. Wu, Q. Meng, C. Yang, Q. Zhou, Z. Feng, D. Zhu, Abnormal carbon and hydrogen isotopes of alkane gases from the Qingshen gas field, Songliao Basin, China, suggesting abiogenic alkanes? *J. Asian Earth Sci.* **115**, 285–297 (2016).
65. J. Horita, M. E. Berndt, Abiogenic methane formation and isotopic fractionation under hydrothermal conditions. *Science* **285**, 1055–1057 (1999).
66. A. Cheng, B. Sherwood Lollar, J. G. Gluyas, C. J. Ballentine, Primary N_2–He gas field formation in intracratonic sedimentary basins. *Nature* **615**, 94–99 (2023).
67. L.-H. Lin, J. Hall, J. Lippmann-Pipke, J. A. Ward, B. Sherwood Lollar, M. DeFlaun, R. Rothmel, D. Moser, T. M. Gihring, B. Mislowack, T. C. Onstott, Radiolytic H_2 in continental crust: Nuclear power for deep subsurface microbial communities. *Geochem. Geophys. Geosyst.* **6**, Q07003 (2005).
68. L.-H. Lin, G. F. Slater, B. Sherwood Lollar, G. Lacrampe-Couloume, T. C. Onstott, The yield and isotopic composition of radiolytic H_2, a potential energy source for the deep subsurface biosphere. *Geochim. Cosmochim. Acta* **69**, 893–903 (2005).
69. Z. Feng, C. Yin, J. Qi, J. Dong, Main factors controlling hydrocarbon accumulation in large volcanic gas fields: A case study of the Qingshen gas field in the Songliao basin. *Acta Petrol. Sin.* **26**, 21–32 (2010).
70. N. H. Sleep, D. K. Bird, Niches of the pre-photosynthetic biosphere and geologic preservation of Earth's earliest ecology. *Geobiology* **5**, 101–117 (2007).
71. T. Wang, C. Wang, J. Ramezani, X. Wan, Z. Yu, Y. Gao, H. He, H. Wu, High-precision geochronology of the Early Cretaceous Yingcheng Formation and its stratigraphic implications for Songliao Basin, China. *Geosci. Front.* **13**, 101386 (2022).
72. L. Zhang, Z. Wang, B. Xu, H. Zou, P. Zhao, H. Zhang, Neoproterozoic–Early Cambrian igneous and sedimentary sequences in the Songliao Block, NE China: Records of Rodinia supercontinent evolution in eastern Central Asian orogenic Belt. *Precambrian Res.* **381**, 106865 (2022).
73. F. Gaillard, M. A. Bouhifd, E. Füri, V. Malavergne, Y. Marrocchi, L. Noack, G. Ortenzi, M. Roskosz, S. Vulpius, The diverse planetary ingassing/outgassing paths produced over billions of years of magmatic activity. *Space Sci. Rev.* **217**, 22 (2021).
74. B. Marty, G. Avice, Y. Sano, K. Altwegg, H. Balsiger, M. Hässig, A. Morbidelli, O. Mousis, M. Rubin, Origins of volatile elements (H, C, N, noble gases) on Earth and Mars in light of recent results from the ROSETTA cometary mission. *Earth Planet. Sci. Lett.* **441**, 91–102 (2016).
75. Y. Shuai, G. Etiope, S. C. Zhang, P. M. J. Douglas, L. Huang, J. M. Eiler, Methane clumped isotopes in the Songliao Basin (China): New insights into abiotic vs. biotic hydrocarbon formation. *Earth Planet. Sci. Lett.* **482**, 213–221 (2018).
76. F. Zhang, H. Chen, X. Yu, C. Dong, S. Yang, Y. Pang, G. E. Batt, Early Cretaceous volcanism in the northern Songliao Basin, NE China, and its geodynamic implication. *Gondw. Res.* **19**, 163–176 (2011).
77. Y. Hao, Z. Pang, J. Tian, Y. Wang, Z. Li, L. Li, L. Xing, Origin and evolution of hydrogen-rich gas discharges from a hot spring in the eastern coastal area of China. *Chem. Geol.* **538**, 119477 (2020).
78. K. Suda, Y. Ueno, M. Yoshizaki, H. Nakamura, K. Kurokawa, E. Nishiyama, K. Yoshino, Y. Hongoh, K. Kawachi, S. Omori, K. Yamada, N. Yoshida, S. Maruyama, Origin of methane in serpentinite-hosted hydrothermal systems: The CH_4–H_2–H_2O hydrogen isotope systematics of the Hakuba Happo hot spring. *Earth Planet. Sci. Lett.* **386**, 112–125 (2014).
79. W. Zhao, Z. Guo, M. Lei, M. Zhang, L. Ma, D. Fortin, G. Zheng, Volcanogenic CO_2 degassing in the songliao continental rift system, NE China. *Geofluids* **2019**, 1–14 (2019).
80. X. Liu, X. Fu, D. Liu, W. Wei, X. Lu, C. Liu, W. Wang, H. Gao, Distribution of mantle-derived CO_2 gas reservoir and its relationship with basement faults in Songliao Basin, China. *J. Nat. Gas Sci. Eng.* **56**, 593–607 (2018).
81. Y. Liu, S. Xie, G. Feng, C. Su, Q. Xu, T. Gao, Evolution of kerogen structure during the carbonization stage. *Org. Geochem.* **190**, 104743 (2024).
82. J. Dai, J. Li, X. Luo, W. Zhang, G. Hu, C. Ma, J. Guo, S. Ge, Stable carbon isotope compositions and source rock geochemistry of the giant gas accumulations in the Ordos Basin, China. *Org. Geochem.* **36**, 1617–1635 (2005).
83. J. A. Welhan, H. Craig, Methane and hydrogen in East Pacific Rise hydrothermal fluids. *Geophys. Res. Lett.* **6**, 829–831 (1979).
84. J. Dai, C. Zou, S. Zhang, J. Li, Y. Ni, G. Hu, X. Luo, S. Tao, G. Zhu, J. Mi, Z. Li, A. Hu, C. Yang, Q. Zhou, Y. Shuai, Y. Zhang, C. Ma, Discrimination of abiogenic and biogenic alkane gases. *Sci. China, Ser. D: Earth Sci.* **51**, 1737–1749 (2008).
85. Y. Li, R. Gao, J. Yao, S. Mi, W. Li, X. Xiong, J. Gao, The crust velocity structure of Da Hinggan Ling orgenic belt and the basins on both sides. *Prog. Geophys.* **29**, 73–83 (2014).
86. Z. Li, Y. Yan, Characteristics of radiogenic heat of the Jurassic in Songliao Basin and its significance. *Geotecton. Metallog.* **26**, 297–299 (2002).
87. S. Zhang, C. Zou, C. Peng, J. Zhao, N. Li, X. Zhang, H. Ma, Y. Niu, Abnormally high natural radioactivity zones in the main borehole of the Continental Scientific Drilling Project of Cretaceous Songliao Basin: Geophysical log responses and genesis analysis. *Chin. J. Geophys.* **61**, 4712–4728 (2018).
88. S. Dai, L. Wang, Z. Xin, Testing and characteristic analysis of elastic parameters of basement rock in the paleo-central uplift belt in the northern Songliao Basin. *Oil Geophys. Prospect.* **58**, 443–453 (2023).
89. C. M. Bethke, A numerical model of compaction-driven groundwater flow and heat transfer and its application to the paleohydrology of intracratonic sedimentary basins. *J. Geophys. Res. Solid Earth* **90**, 6817–6828 (1985).
90. S. Gao, T. Luo, B. Zhang, H. Zhang, Y. Han, Z. Zhao, H. Kern, Structure and composition of the continental crust in East China. *Sci. China, Ser. D: Earth Sci.* **42**, 129–140 (1999).
91. R. M. Coveney, E. D. Goebel, E. J. Zeller, G. A. M. Dreschhoff, E. E. Angino, Serpentinization and the origin of hydrogen gas in Kansas. *AAPG Bull.* **71**, 39–48 (1987).
92. T. A. Abrajano, N. C. Sturchio, J. K. Bohlke, G. L. Lyon, R. J. Poreda, C. M. Stevens, Methane-hydrogen gas seeps, Zambales Ophiolite, Philippines: Deep or shallow origin? *Chem. Geol.* **71**, 211–222 (1988).
93. Z. Shangguan, W. Huo, δD values of escaped H_2 from hot springs at the Tengchong Rehai geothermal area and its origin. *Chin. Sci. Bull.* **47**, 148–150 (2002).
94. Y. Shuai, S. Zhang, A. Su, H. Wang, B. Cai, H. Wang, Geochemical evidence for strong ongoing methanogenesis in Sanhu region of Qaidam Basin. *Sci. China Ser. D: Earth Sci.* **53**, 84–90 (2009).
95. G. Etiope, N. Samardžić, F. Grassa, H. Hrvatović, N. Miošić, F. Skopljak, Methane and hydrogen in hyperalkaline groundwaters of the serpentinized Dinaride ophiolite belt, Bosnia and Herzegovina. *Appl. Geochem.* **84**, 286–296 (2017).
96. N. Suzuki, H. Saito, T. Hoshino, Hydrogen gas of organic origin in shales and metapelites. *Int. J. Coal Geol.* **173**, 227–236 (2017).
97. X. Zhai, L. Yang, X. Xue, Y. Gao, P. Wang, Prediction of the bottom hole geotemperature, formation pressure and formation fracture pressure of the Continental Scientific Drilling of Cretaceous Songliao Basin (SK2). *Earth Sci. Front.* **24**, 257–264 (2017).
98. J. Han, Z. Guo, W. Liu, H. Hou, G. Liu, S. Han, L. Liu, T. Wang, Deep dynamic process of lithosphere thinning in Songliao basin. *Chin. J. Geophys.* **61**, 2265–2279 (2018).
99. Y. Hao, X. Kuang, Y. Feng, Y. Wang, H. Zhou, C. Zheng, Discovery and genesis of helium-rich geothermal fluids along the India–Asia continental convergent margin. *Geochim. Cosmochim. Acta* **360**, 175–191 (2023).
100. J. Dai, G. Hu, Y. Ni, J. Li, X. Luo, C. Yang, A. Hu, Q. Zhou, Natural gas accumulation in Eastern China. *Energy Explor. Exploit.* **27**, 225–259 (2009).
101. D. Xiao, S. Lu, M. Shao, N. Zhou, R. Zhao, Y. Peng, Comparison of marine and continental shale gas reservoirs and their gas-bearing properties in China: The examples of the longmaxi and shahezi shales. *Energy Fuel* **35**, 4029–4043 (2021).
102. M. J. Whiticar, Carbon and hydrogen isotope systematics of bacterial formation and oxidation of methane. *Chem. Geol.* **161**, 291–314 (1999).
103. H. Hosgormez, G. Etiope, M. N. YalÇIn, New evidence for a mixed inorganic and organic origin of the Olympic Chimaera fire (Turkey): A large onshore seepage of abiogenic gas. *Geofluids* **8**, 263–273 (2008).
104. B. Sherwood Lollar, S. K. Frape, P. Fritz, S. A. Macko, J. A. Welhan, R. Blomqvist, P. W. Lahermo, Evidence for bacterially generated hydrocarbon gas in Canadian shield and fennoscandian shield rocks. *Geochim. Cosmochim. Acta* **57**, 5073–5085 (1993).
105. B. Sherwood Lollar, S. K. Frape, S. M. Weise, P. Fritz, S. A. Macko, J. A. Welhan, Abiogenic methanogenesis in crystalline rocks. *Geochim. Cosmochim. Acta* **57**, 5087–5097 (1993).
106. Y. Sano, B. Marty, Origin of carbon in fumarolic gas from island arcs. *Chem. Geol.* **119**, 265–274 (1995).
107. B. Marty, A. Jambon, C^3He in volatile fluxes from the solid Earth: implications for carbon geodynamics. *Earth Planet. Sci. Lett.* **83**, 16–26 (1987).

Acknowledgments: All the samples were collected from the PetroChina Daqing Oilfield Co. Ltd., and the natural gas composition and isotopes were measured at the Northwest Institute of Eco-Environment and Resources, Chinese Academy of Sciences. This work has benefited greatly from discussions on isotopes with W. Li from SANYA Offshore Oil and Gas Research Institute of Northeast Petroleum University and H. Xie from Nanjing University. **Funding:** This

study was supported by the National Natural Science Foundation of China (grant nos. 42488101, 42141021, and U20B6001) and Tencent Xplorer Prize. **Author contributions:** Conceptualization: Q.L., Z.J., Y.W., P.L., and W.Z. Methodology: Q.L., Y.W., X.W., and Dongya Zhu. Validation: H.X., Di Zhu, and Q.L. Formal analysis: Y.W., Q.M., and H.X. Investigation: Q.L., Y.W., and X.H. Resources: Q.L., X.W., Dongya Zhu, and W.Z. Data curation: Y.W., Y.F., and Q.M. Writing—original draft: Q.L., Y.W., and X.W. Writing—review and editing: Q.L., X.W., Z.J., and Dongya Zhu. Visualization: Y.W., P.L., and X.W. Supervision: Q.L., W.Z., Di Zhu, and X.W. Project administration: Q.L., Y.W., and Q.M. Funding acquisition: Q.L. Z.J., and W.Z. **Competing interests:** The authors declare that they have no competing interests. **Data and materials availability:** All data needed to evaluate the conclusions in the paper and/or the Supplementary Materials.

Submitted 12 July 2024
Accepted 23 December 2024
Published 24 January 2025
10.1126/sciadv.adr6771